Electronic Supplementary Material (ESI) for Journal of Materials Chemistry B.

Electronic Supplementary Information

Combining surface chemistry modification and in situ small-angle scattering characterization to understand and optimize the biological behavior of nanomedicines

Marine Le Goas,* Tom Roussel, Maria Kalbazova, David Carrière, Elodie Barruet, Valerie Geertsen, Giulia Fadda, Fabienne Testard, Geraldine Carrot* and Jean-Philippe Renault*

Scheme S1. Synthesis reactions of polymethacrylate ligands and polymer-grafted gold nanoparticles (A) P*t*BuMA synthesis through ATRP (B) Hydrolysis of *t*BuMA units (C) PMAA-AuNPs direct synthesis.

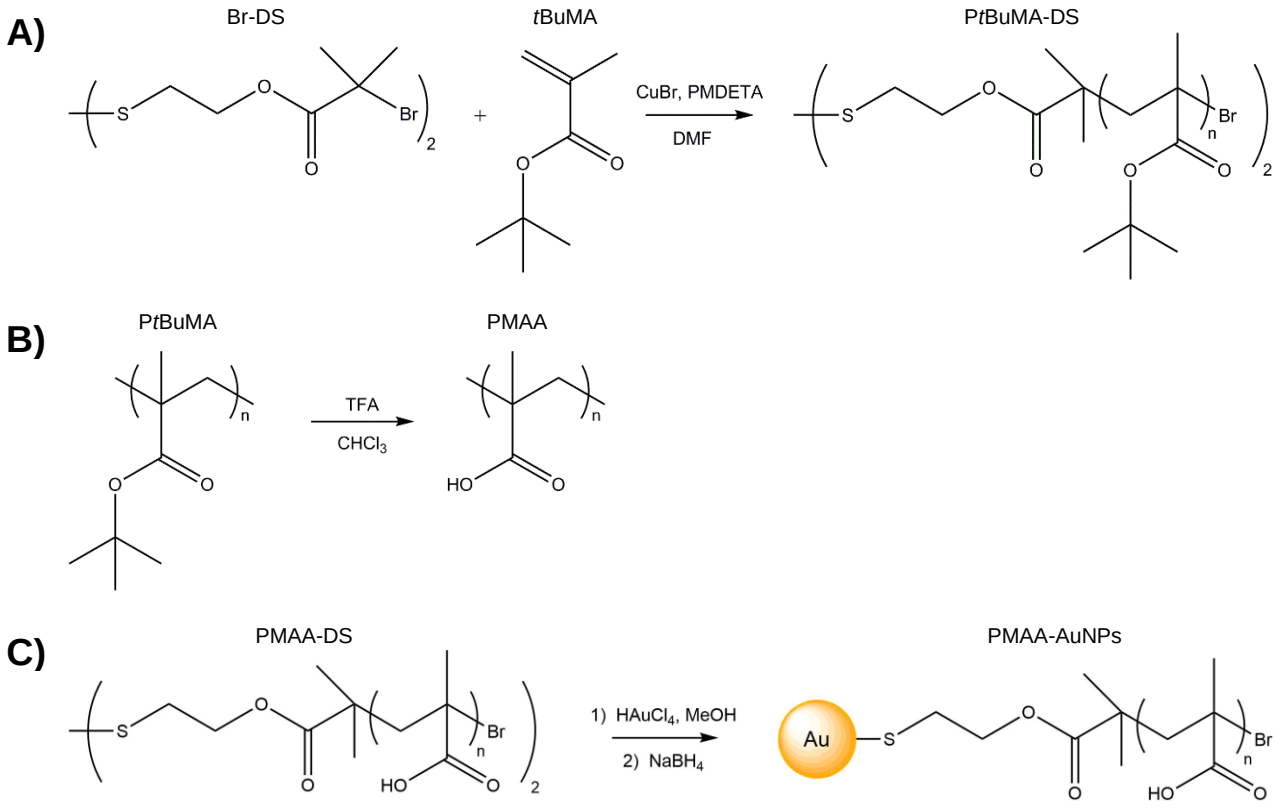

Table S1. Summary of polymers characteristics.

Polymer	Theoretical Mn (kg/mol)	%v DMF / T (°C)	Conversion rate (%)	SEC analysis before hydrolysis (THF)		Hydrolysis rate (%) (from NMR data)	SEC analysis after hydrolysis (phosphate)		Number of monomer units (calculated after hydrolysis)	% other monomer (from NMR data)
				Mn (kg/mol)	Ip		Mn (kg/mol)	Ip		
PMAA-DS	40	32% 60°C	70	/	/	98	21.1	1.3	242	/
PMAA-DS	40	32% 60°C	51.8	21.9	1.1	98.4	14.8	1.2	169	/
PMAA-DS	106	10% 60°C	58.4	55.3	1.2	98.0	37.1	1.2	428	/
PDMAEMA-DS	40	0% 25°C	98.0	43.8	1.2	/	/	/	277	/
P(DMAEMA-MAA)-DS (10/90)	40	32% 60°C	48.2	20.5	1.3	98.0	15.9	1.3	168	10.0
P(*n*BuMA-MAA)-DS (20/80)	40	17% 60°C	77.4	34.5	1.3	97.8	21.0 (NMR)	/	241	22.5
P(PEGMA-MAA)-DS (10/90)	40	32% 60°C	/	49.7	3.0	98.1	44.2	1.9	392	9.5
P(HEMA-MAA)-DS (50/50)	15	38% 60°C	45	/	/	95.3	/	/	/	48.0

Figure S1. [1]H NMR spectra of polymeric ligands before (a) and after (b) hydrolysis. (A) PMAA-DS (B) PDMAEMA-DS (C) P(DMAEMA-MAA)-DS (D) P(*n*BuMA-MAA)-DS (E) P(PEGMA-MAA)-DS (F) P(HEMA-MAA)-DS.

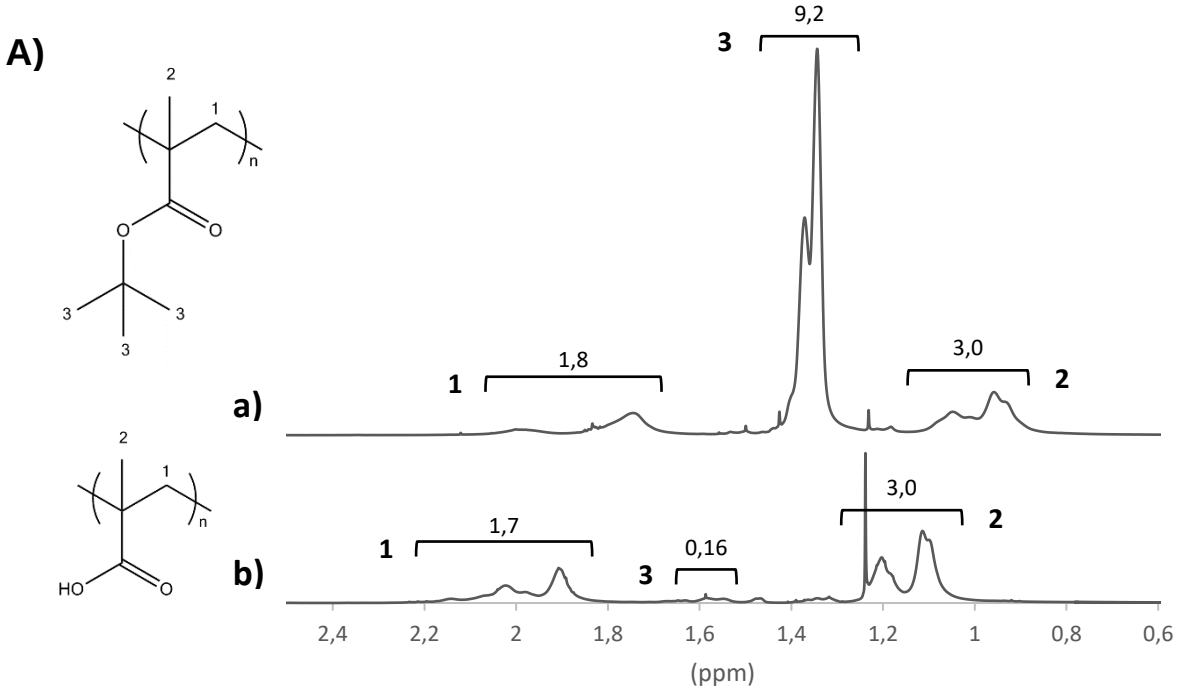

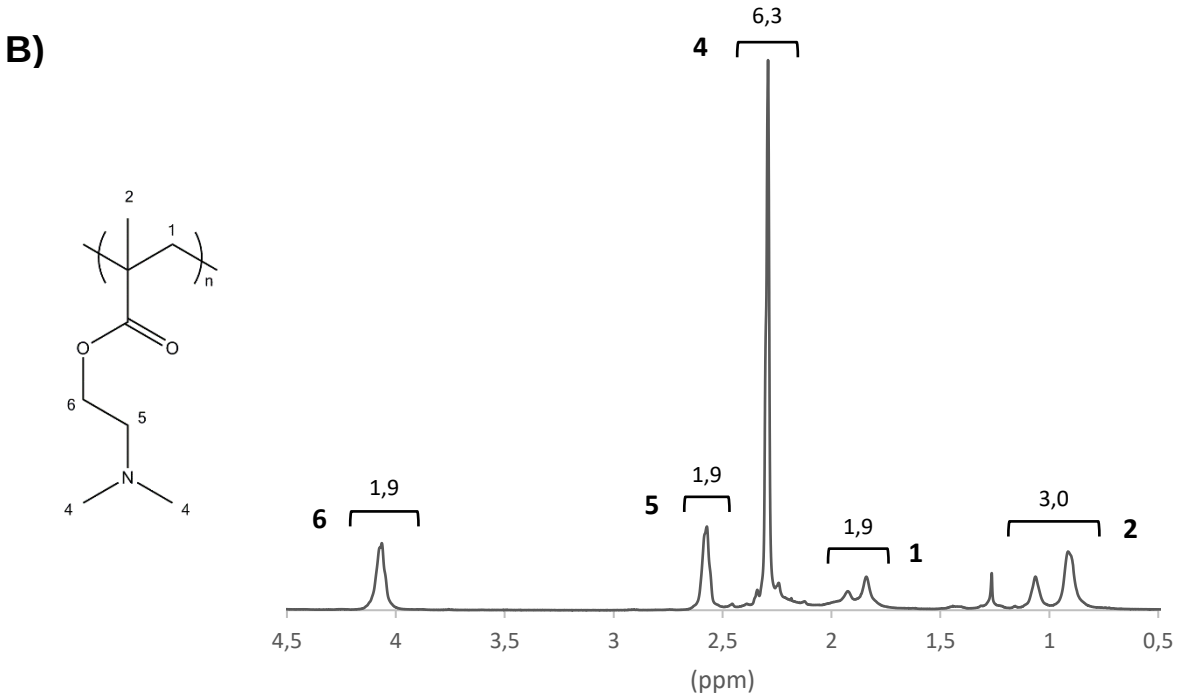

C)

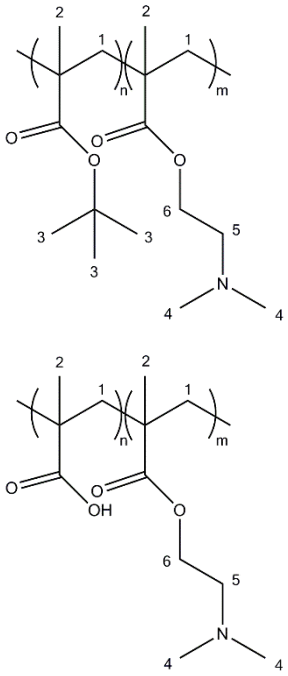

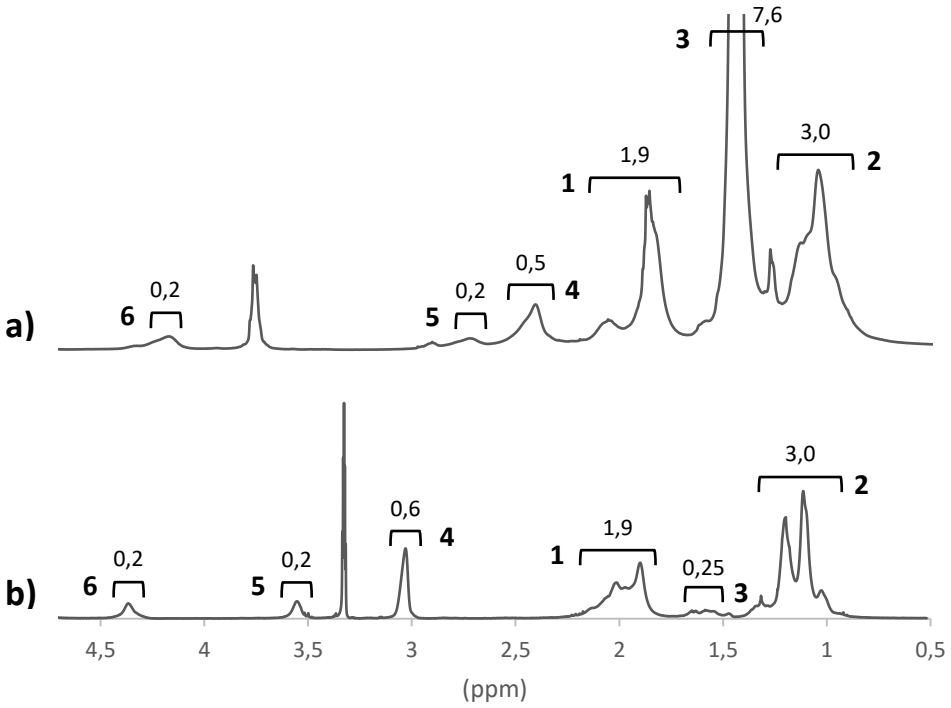
a)
6 0,2
5 0,2
4 0,5
1 1,9
3 7,6
2 3,0
b)
6 0,2
5 0,2
4 0,6
1 1,9
0,25
3
2 3,0
4,5 4 3,5 3 2,5 2 1,5 1 0,5
(ppm)

D)

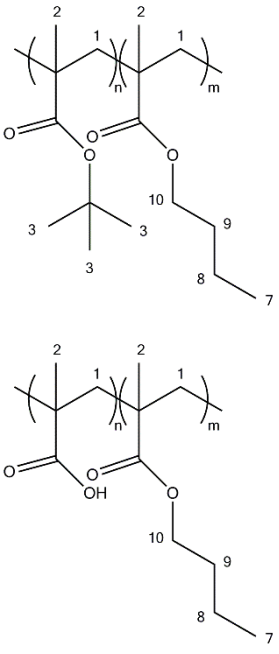

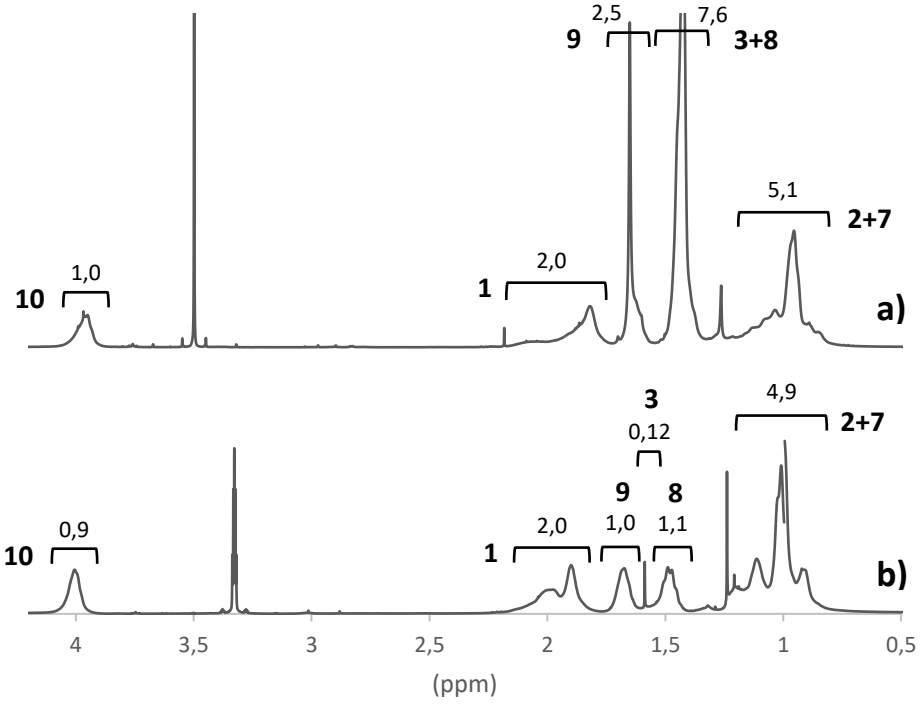
a)
10 1,0
1 2,0
9 2,5
3+8 7,6
2+7 5,1
b)
10 0,9
1 2,0
9 1,0
8 1,1
3 0,12
2+7 4,9
4 3,5 3 2,5 2 1,5 1 0,5
(ppm)

E)

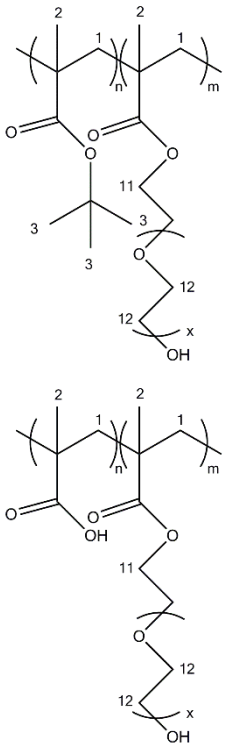

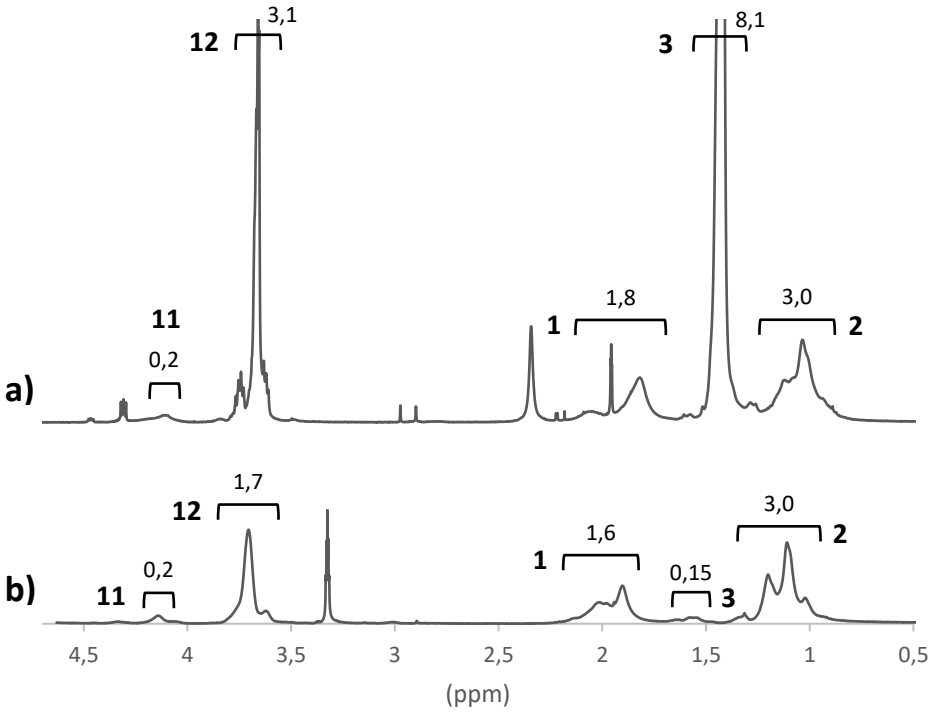
12
3,1
3
8,1
11
0,2
1
1,8
3,0
2
a)
12
1,7
1
1,6
3,0
2
11
0,2
0,15
3
b)
4,5
4
3,5
3
2,5
2
1,5
1
0,5
(ppm)

F)

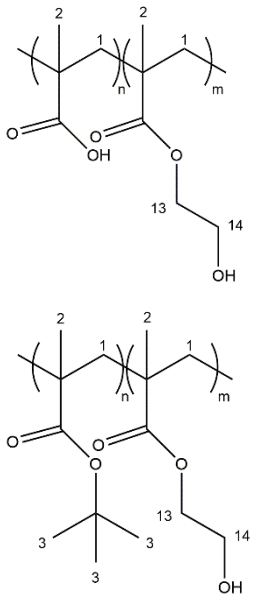

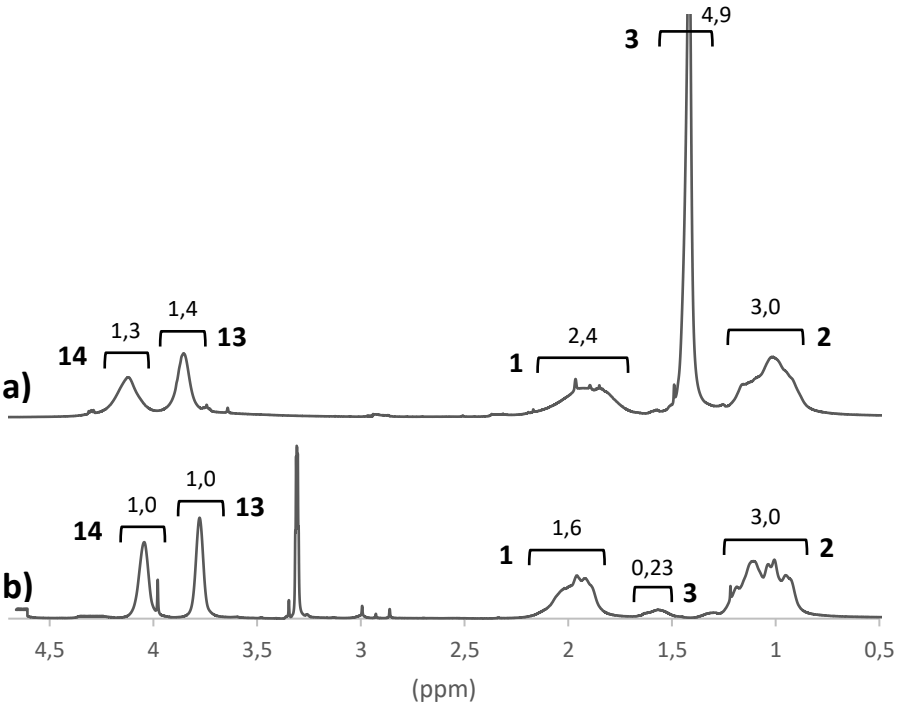
3
4,9
14
1,3
1,4
13
1
2,4
3,0
2
a)
14
1,0
1,0
13
1
1,6
3,0
2
0,23
3
b)
4,5
4
3,5
3
2,5
2
1,5
1
0,5
(ppm)

Figure S2. UV-visible spectra of NPs. (A) PMAA(7)-AuNPs, PMAA(11)-AuNPs and PMAA(19)-AuNPs (B) PDMAEMA-AuNPs and P(DMAEMA-MAA-AuNPs (C) P(HEMA-MAA)-AuNPs, P(*n*BuMA-MAA)-AuNPs and P(PEGMA-MAA)-AuNPs.

Absorption spectra were recorded using a Shimadzu UV-2450 double-beam UV–Vis spectrophotometer.

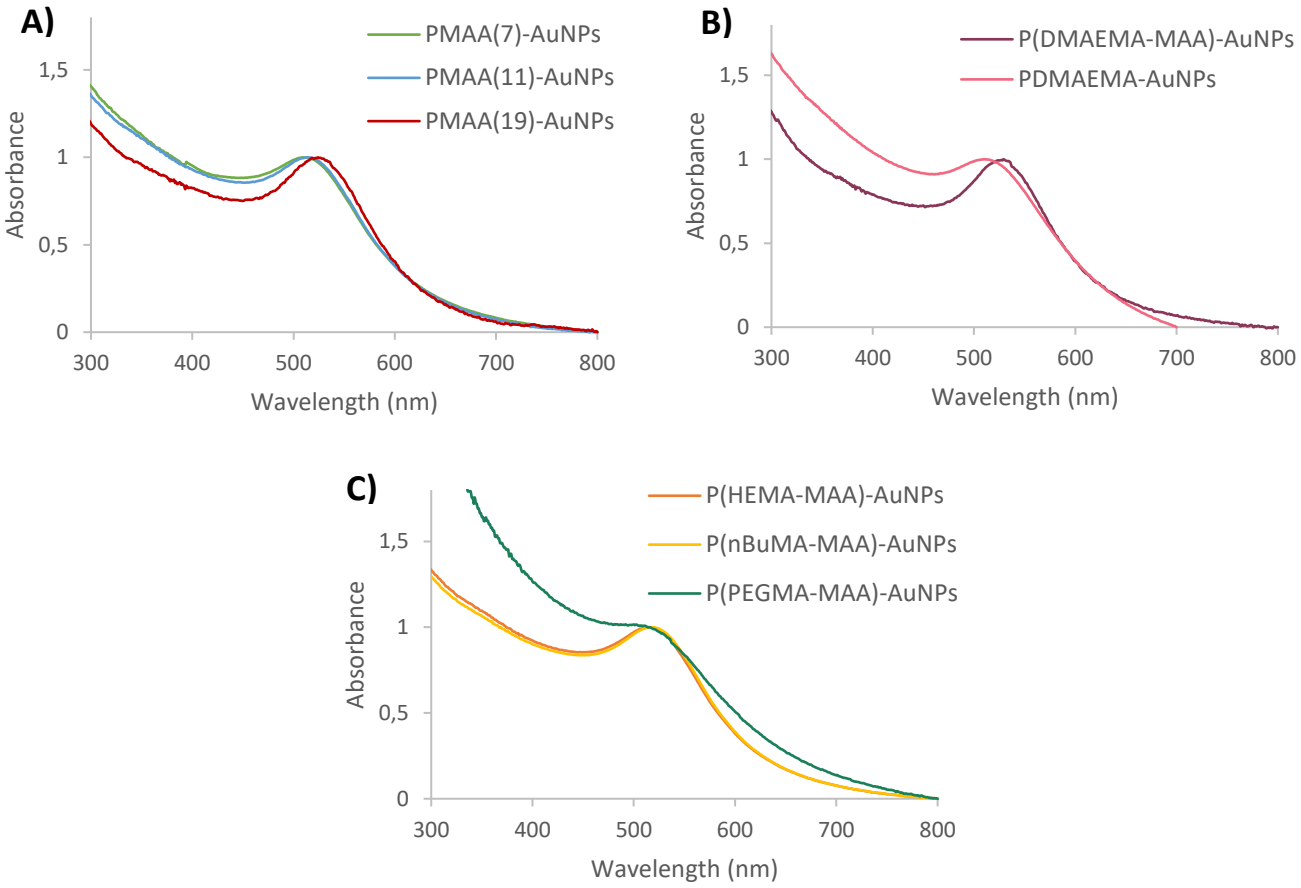

Table S2. X-ray scattering length densities of the compounds used in this study.

Compound	ρ_{SAXS} (10^6 Å^{-2})	
	8 keV (XEUSS)	**16 keV (SWING beamline)**
Gold	124.89	126.58
MAA	9.24	9.21
HEMA	9.83	9.80
DMAEMA	8.69	8.67
*n*BuMA	8.35	8.33
PEGMA (Mn = 360)	10.23	10.20
Water	9.47	9.43

Figure S3. SAXS data of NPs. (A) PMAA(7)-AuNPs (B) PMAA(11)-AuNPs (C) PMAA(19)-AuNPs (D) P(HEMA-MAA)-AuNPs (E) PDMAEMA-AuNPs (F) P(*n*BuMA-MAA)-AuNPs (G) P(DMAEMA-MAA)-AuNPs (H) P(PEGMA-MAA)-AuNPs.

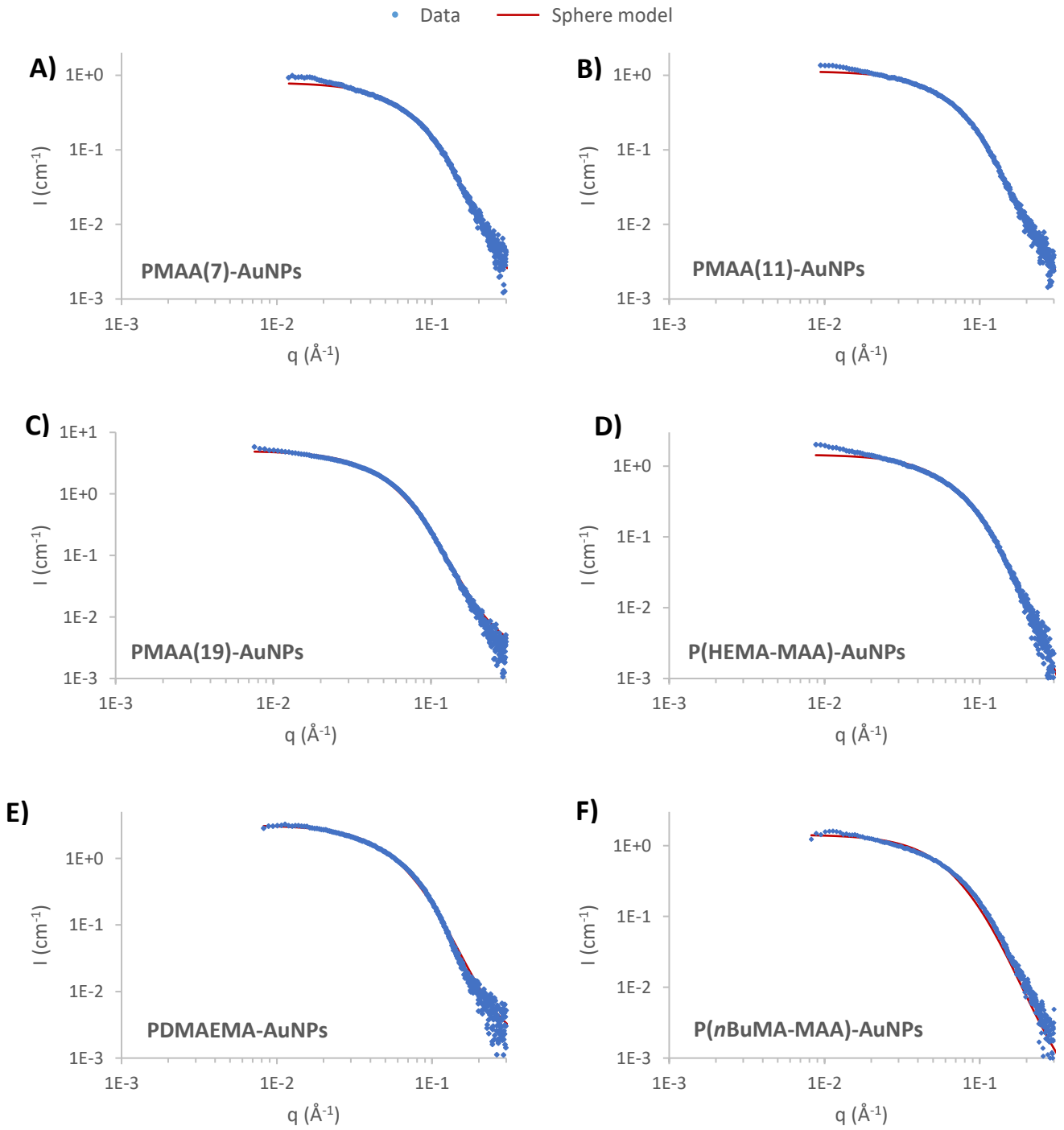

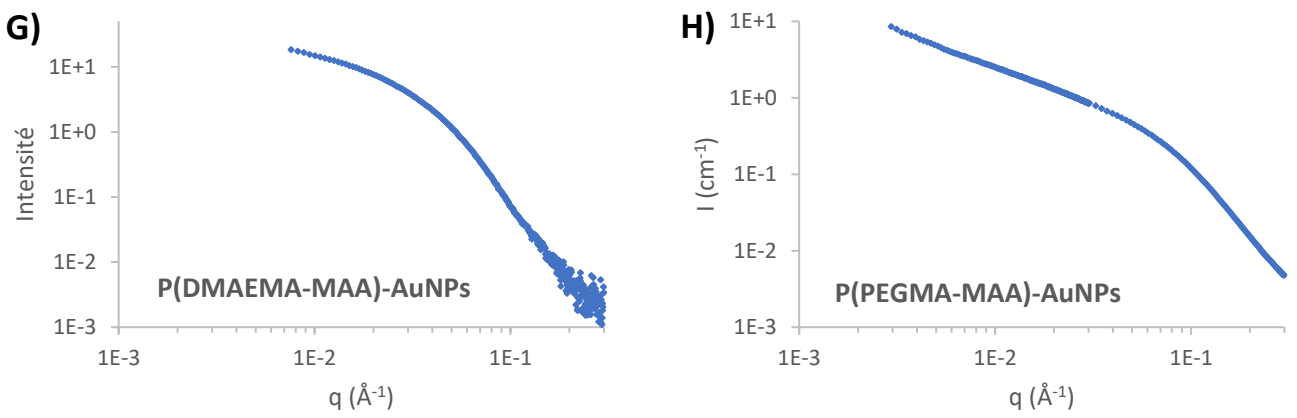

Figure S4. TEM images of NPs. (A) PMAA(7)-AuNPs (B) PMAA(11)-AuNPs (C) PMAA(19)-AuNPs (D) PDMAEMA-AuNPs (E) P(DMAEMA-MAA)-AuNPs (F) P(HEMA-MAA)-AuNPs (G) P(*n*BuMA-MAA)-AuNPs (H) P(PEGMA-MAA)-AuNPs.

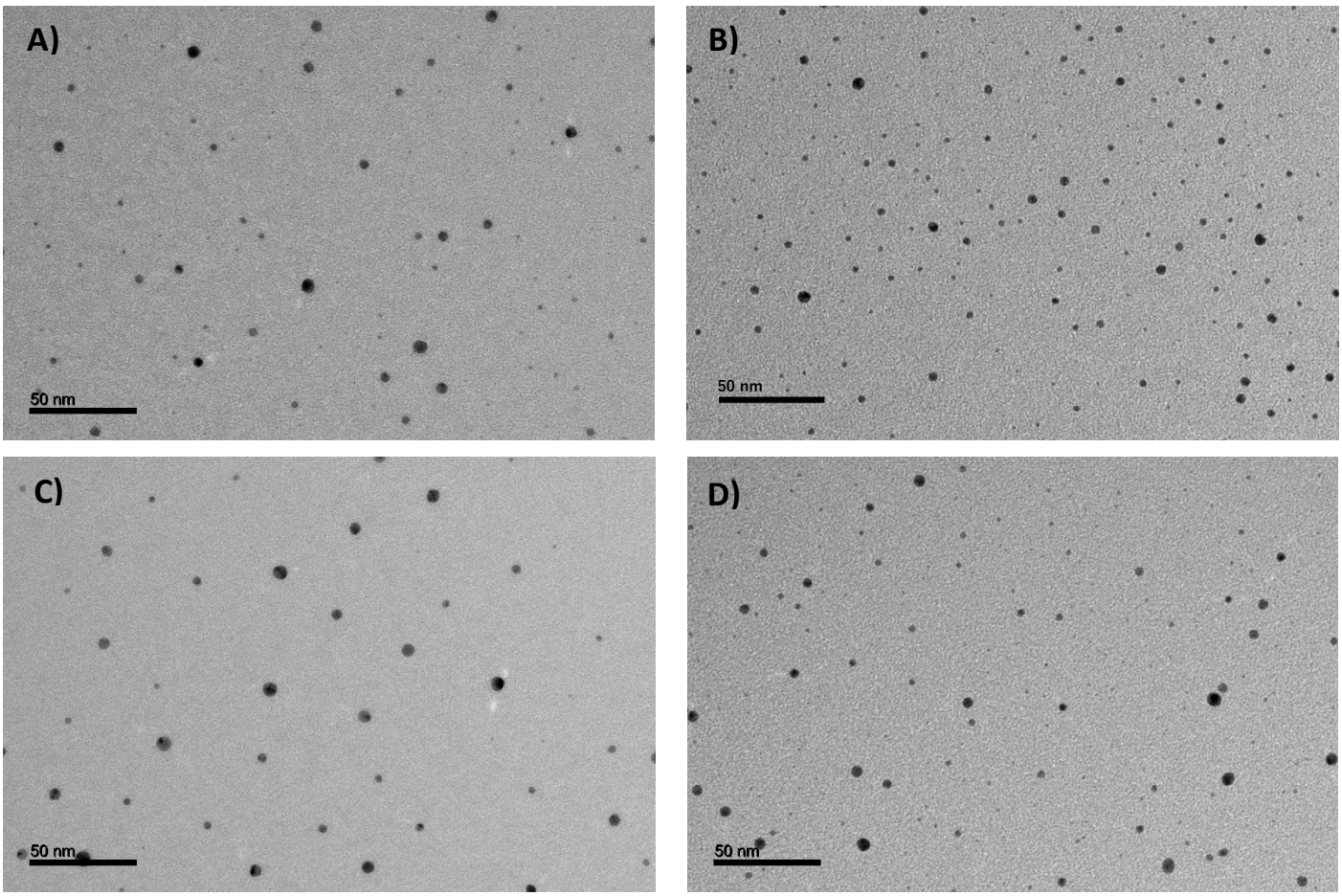

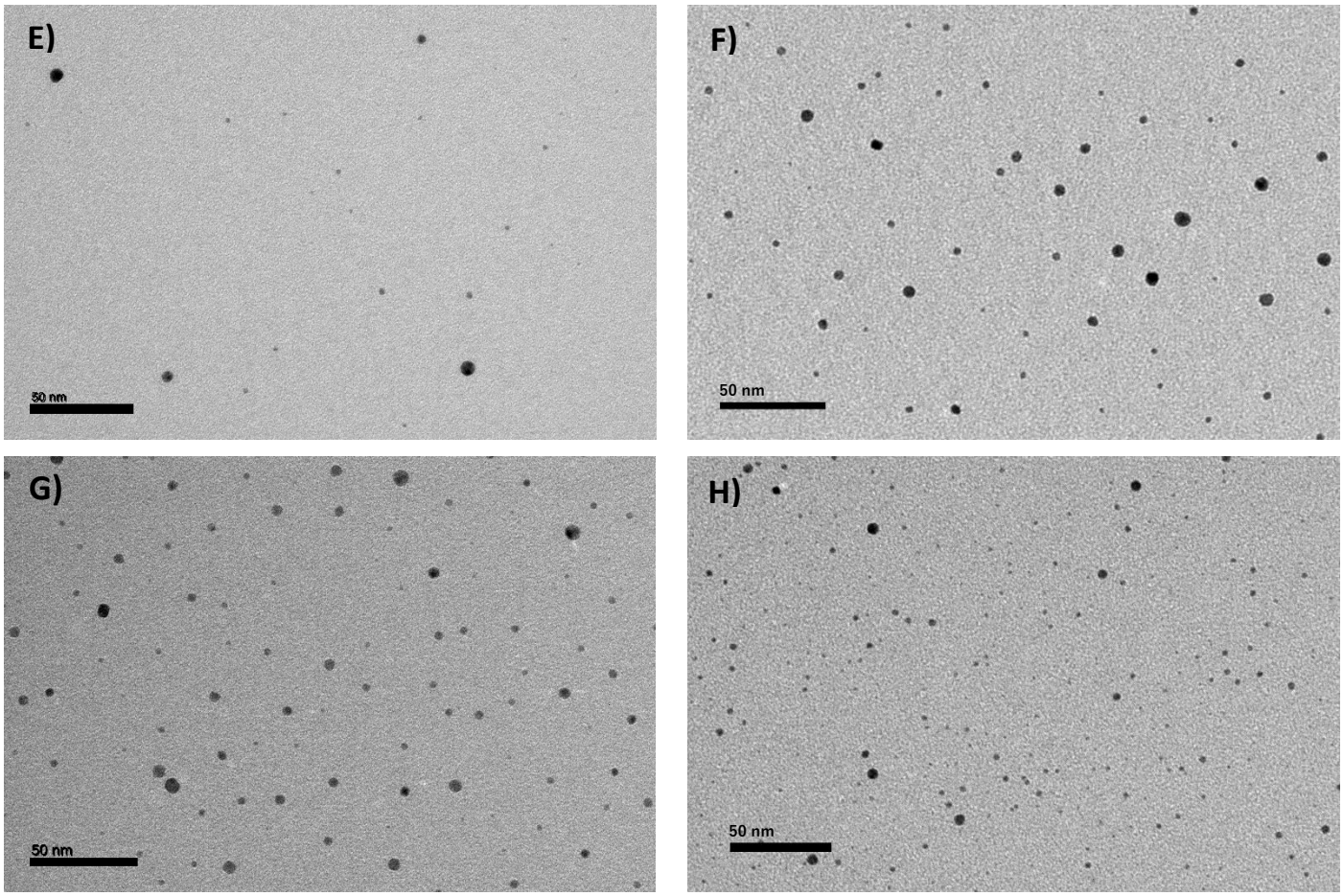

Figure S5. Size diagrams of NPs obtained from TEM and SAXS. (A) PMAA(7)-AuNPs (B) PMAA(11)-AuNPs (C) PMAA(19)-AuNPs (D) PDMAEMA-AuNPs (E) P(DMAEMA-MAA)-AuNPs (F) P(HEMA-MAA)-AuNPs (G) P(*n*BuMA-MAA)-AuNPs (H) P(PEGMA-MAA)-AuNPs.

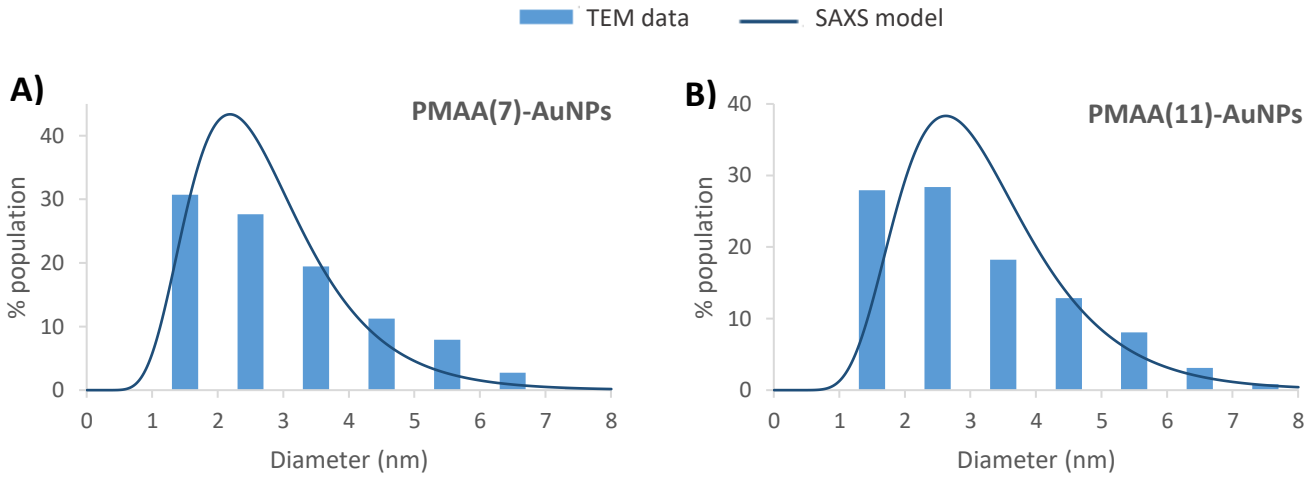

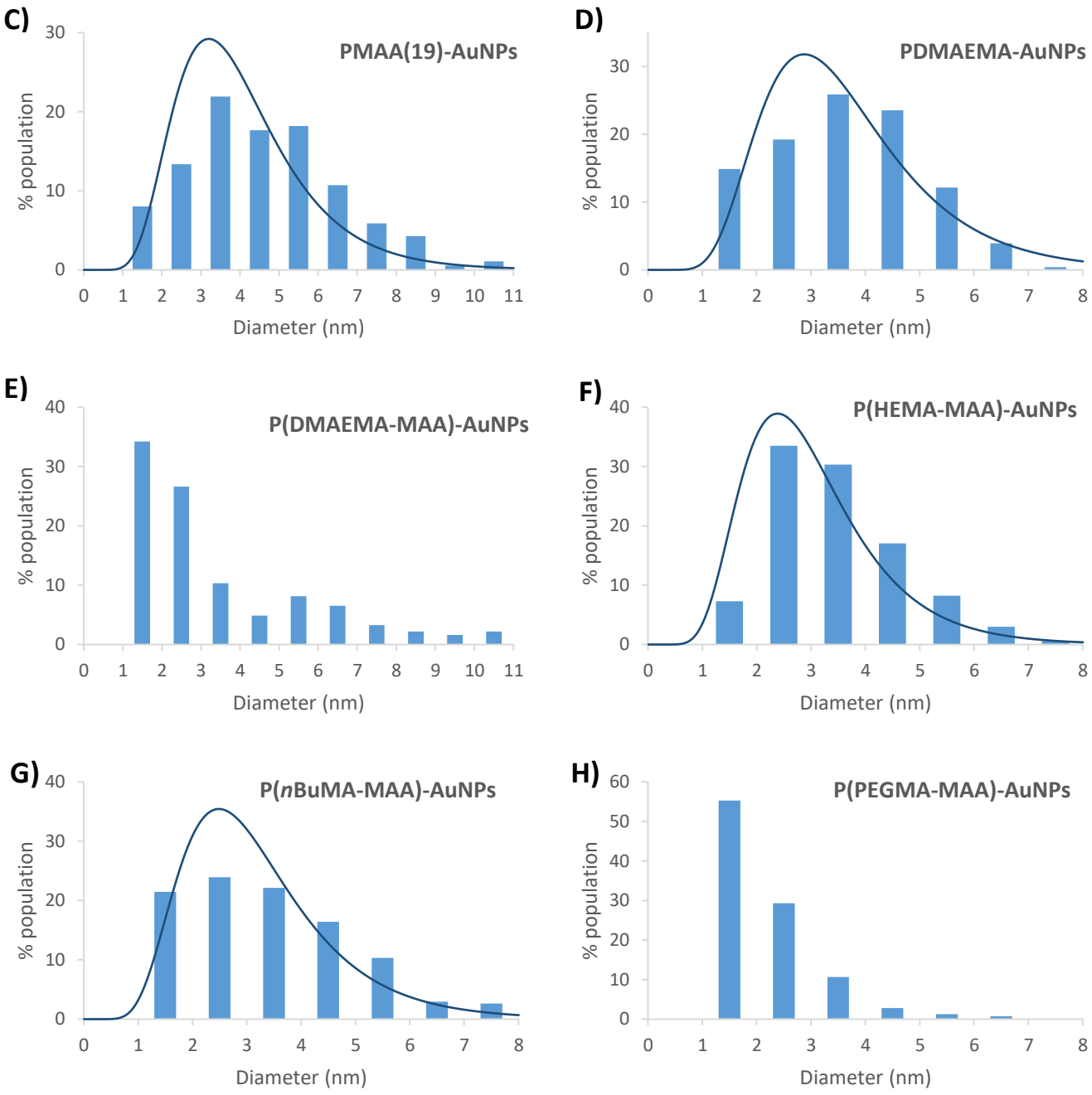

Table S3. Coherent neutron scattering length densities of the compounds used in this study.

Compound	ρ (10^{10} cm^{-2})
H_2O	-0.56
D_2O	6.36
Gold	4.48
PMAA	1.12
PHEMA	0.99
PDMAEMA	0.64
P*n*BuMA	0.47
P(PEGMA)	0.77

Figure S6. SANS data of NPs. (A) PMAA(7)-AuNPs (B) PMAA(11)-AuNPs (C) PMAA(19)-AuNPs (D) P(HEMA-MAA)-AuNPs (E) PDMAEMA-AuNPs (F) P(DMAEMA-MAA)-AuNPs (G) P(PEGMA-MAA)-AuNPs (H) P(*n*BuMA-MAA)-AuNPs.

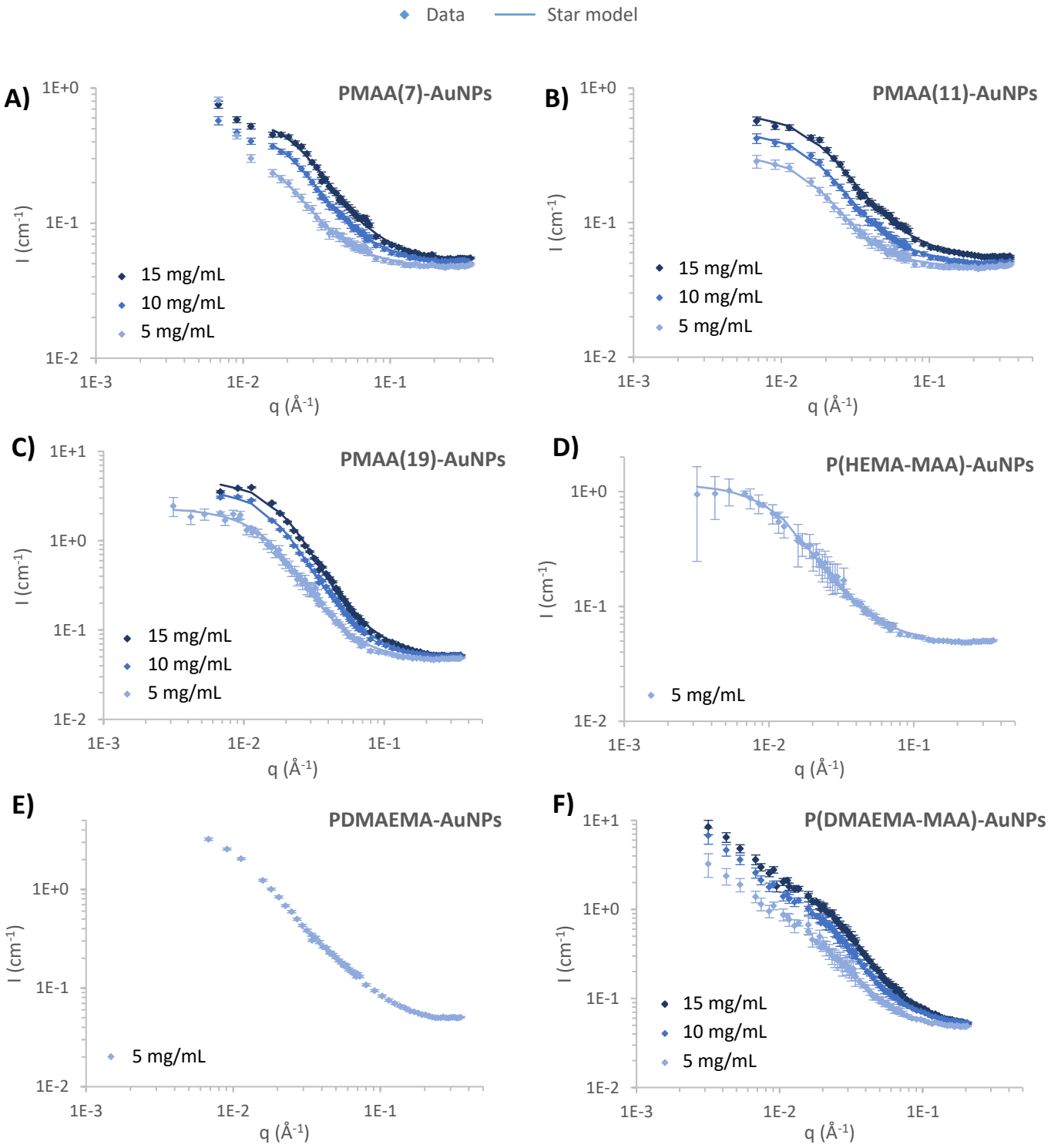

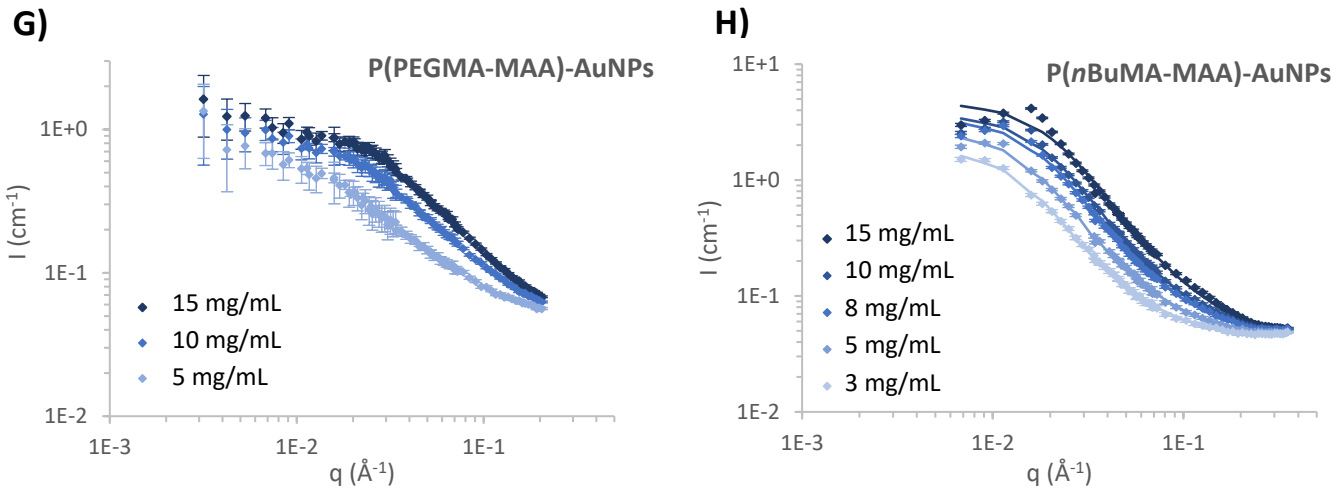

Table S4. Summary of NPs structural characteristics obtained by SANS analysis: Guinier approximation and star model.

NP	Concentration (mg/mL)	$R_g^{Guinier}$ (nm)	R_g^{Star} (nm)	Number of arms	Grafting density (chains/nm^2)
PMAA(7)-AuNPs	10	6.2 ± 0.2	7.4 ± 0.4	3.8 ± 0.5	0.16
PMAA(11)-AuNPs	10	7.3 ± 0.2	8.5 ± 0.4	3.6 ± 0.5	0.11
PMAA(19)-AuNPs	5	12.3 ± 0.2	11.5 ± 0.2	7.4 ± 0.4	0.14
PDMAEMA-AuNPs	/	/	/	/	/
P(DMAEMA-MAA)-AuNPs	/	/	/	/	/
P(HEMA-MAA)-AuNPs	5	11.0 ± 0.3	13.0 ± 0.6	3.5 ± 0.4	0.12
P(*n*BuMA-MAA)-AuNPs	3	9.9 ± 0.2	11.5 ± 0.3	4.2 ± 0.2	0.13
P(PEGMA-MAA)-AuNPs	10	3.7 ± 0.3	/	/	/

Figure S7. Evaluation of colloidal stability of NPs in biological media. SAXS data of NPs in water, DPBS, DMEM, supplemented DMEM and supplemented DMEM exposed to cells. (A) PMAA(11)-AuNPs (B) PMAA(19)-AuNPs (C) P(HEMA-MAA)-AuNPs (D) P(*n*BuMA-MAA)-AuNPs (E) PDMAEMA-AuNPs (F) P(DMAEMA-MAA)-AuNPs (G) P(PEGMA-MAA)-AuNPs.

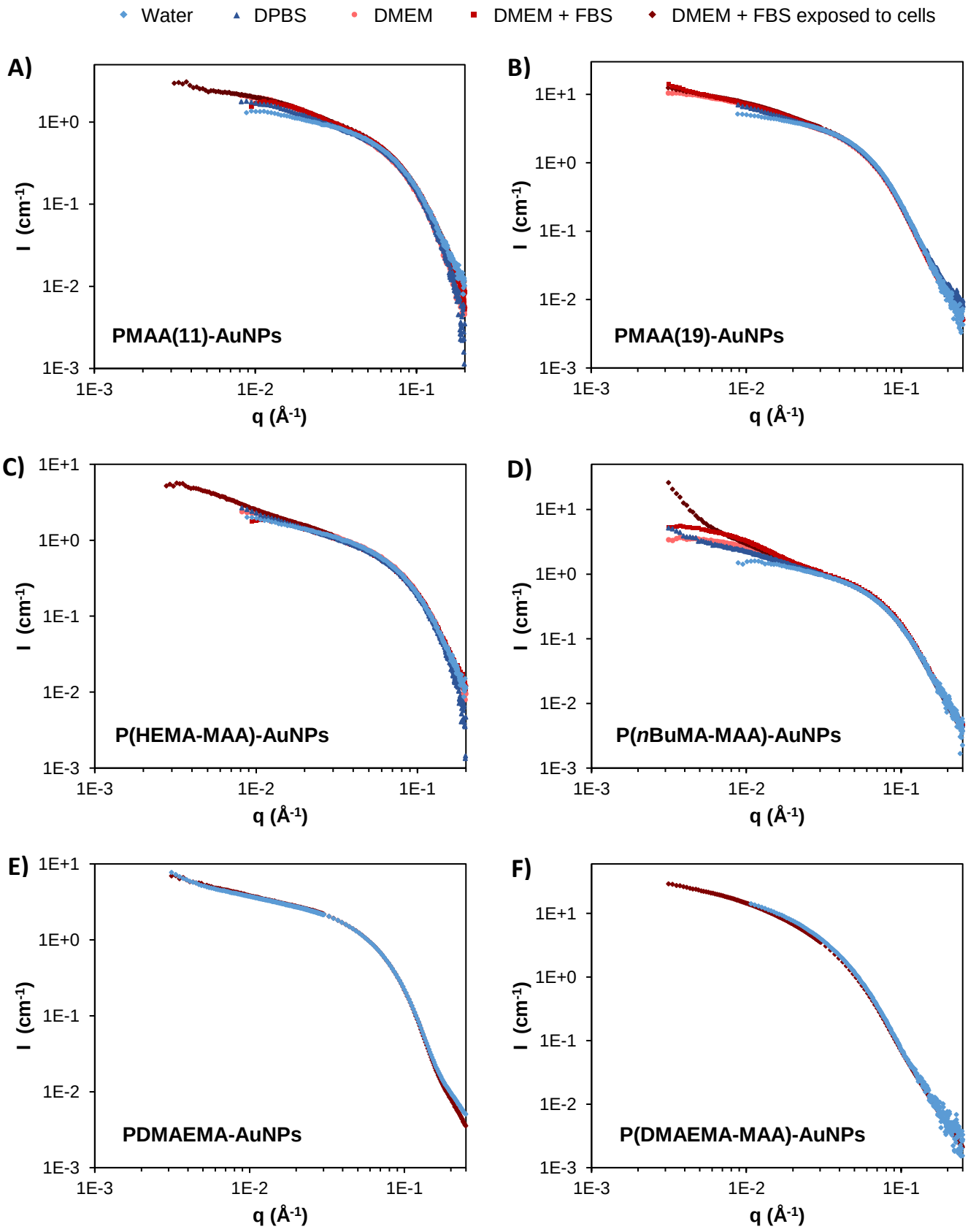

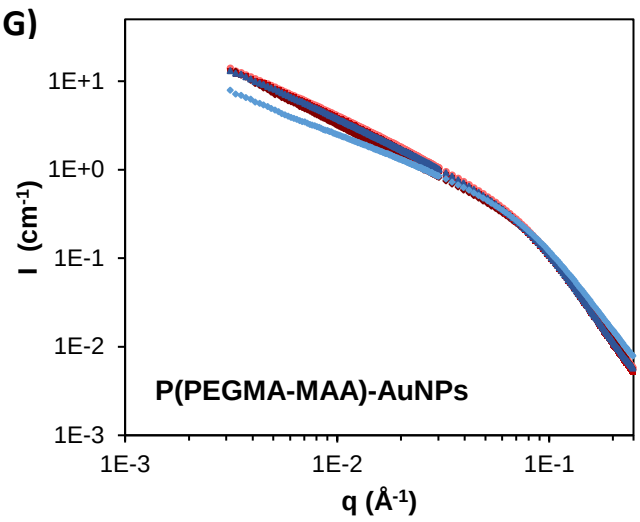

Protocol for cytotoxicity assays. L929 cells were seeded in 96-well plates at a density of 2500 cells/well. After 24 hours, the culture medium was replaced with diluted suspensions (0.1-50 µg/mL Au) of polymer-grafted AuNPs prepared in DMEM supplemented with 10% FBS, 0.25 µg/mL Amphotericin B and 10 µg/mL Gentamicin (only supplemented DMEM was used for controls). Incubation with NPs was performed during 48 hours in order to comply with the norm used to assess cytotoxicity for such nanomaterials (NF EN ISO 10993-5). After the 48-hour exposure, NPs suspensions were removed and 100 µL of clean supplemented DMEM were added in each well, followed by 25 µL of MTT solution (5 mg/mL in PBS) for a 2-hour incubation. Media was then eliminated and 200 µL of DMSO were finally added to dissolve the formazan crystals. Absorbance measurements were taken at 570 nm on a Spectramax Plus 384 (Molecular Devices). To assess reproducibility, 6 wells were used for each condition. Cell viability was calculated as the absorbance ratio between NPs-exposed cells and control (untreated) cells.

Figure S8. Evaluation of the cytotoxicity of NPs. (A) Impact of the polymer length (B) Impact of the nature of polymer (C) Comparison of PDMAEMA-DS and PDMAEMA-AuNPs.

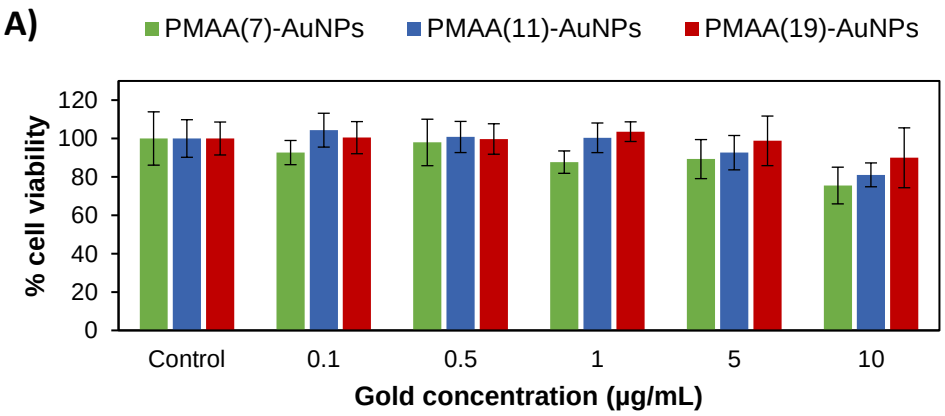

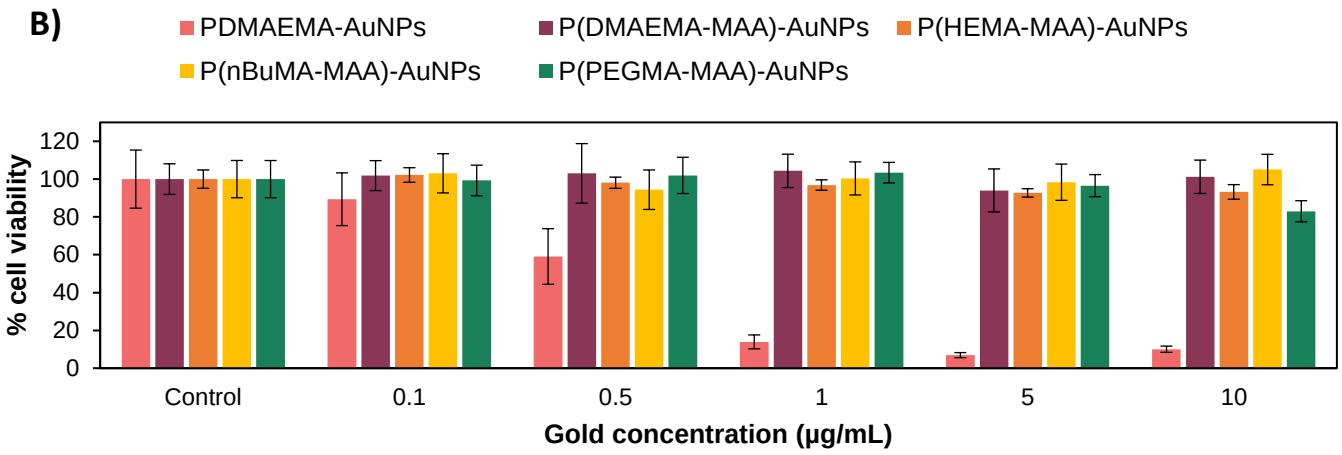

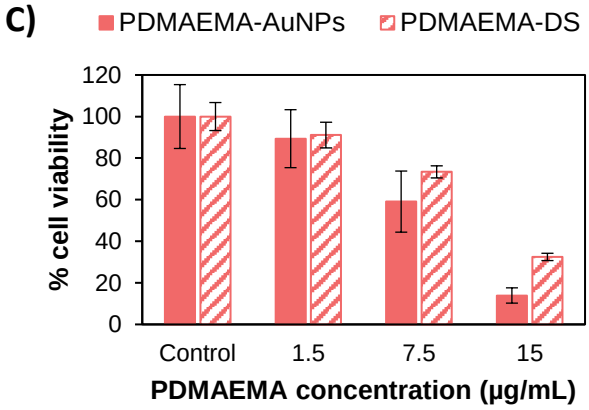

Cytotoxicity assays (MTT) were conducted on non-tumor cells (murine fibroblasts). Conditions of the assay and cell line were chosen to comply with the norm used to assess cytotoxicity for such nanomaterials (NF EN ISO 10993−5).[1] This norm defines a threshold of 70% cell viability under which the product is regarded as toxic.

For all PMAA-AuNPs, whatever PMAA's molecular weight, no toxicity was observed for the range of concentrations considered (Figure S8 A). No statistical difference was either found between the different PMAA lengths. Similar results have been obtained for a range of PEG-covered AuNPs.[2] For other polymethacrylate ligands, most NPs were found to be non-toxic as well (Figure S8 B). Only PDMAEMA-AuNPs showed a marked toxicity from gold concentrations as low as 0.5 µg mL^{-1}.

Cytotoxicity of cationic PDMAEMA was expected, as it has already been shown in the literature.[3,4] Various causes have been suggested, such as disruption of cell membrane, physical rupture of endosomes or perturbation of mitochondria functions, but they are still debated today.[3,5–8] In our case, we tried to determine whether toxicity was only due to PDMAEMA ligands or partly caused by the AuNP itself. Comparison of PDMAEMA-AuNPs with PDMAEMA ligands introduced in the same proportions confirmed the inherent toxicity of PDMAEMA, while showing an additional toxic effect in the case of NPs (Figure S8 C). Gold uptake might play a role in this, but we could also expect that the nanoparticulate structure modified the uptake mechanism and induced different and more toxic phenomena.

Table S5. External and intracellular gold concentrations in cell uptake assays as determined by ICP-MS measurements. Intracellular concentrations were calculated considering a cell volume of 3.4 x 10^{-9} mL with an uncertainty of 10%.[9]

NPs	External gold concentration (μg/mL)	Intracellular gold concentration (μg/mL)	Concentrations ratio
PMAA(7)-AuNPs	0.5	4.1 ± 0.6	7.5
	2.2	5.6 ± 0.8	2.6
	5	6.8 ± 0.9	1.2
	22	10.0 ± 1.5	0.5
PMAA(11)-AuNPs	0.5	6.3 ± 0.7	11.5
	2.2	7.2 ± 0.8	3.3
	5	8.2 ± 0.6	1.5
	22	12.0 ± 1.7	0.6
PMAA(19)-AuNPs	0.5	12.5 ± 2.1	22.9
	2.2	13.2 ± 1.5	6.1
	5	14.7 ± 0.9	2.7
	22	16.3 ± 1.8	0.7
P(HEMA-MAA)-AuNPs	0.5	0.7 ± 0.3	1.2
	2.2	1.0 ± 0.2	0.4
	5	1.8 ± 0.3	0.3
	22	5.9 ± 0.9	0.3
PDMAEMA-AuNPs	0.5	44.9 ± 3.2	82.3
P(*n*BuMA-MAA)-AuNPs	0.5	3.1 ± 0.2	5.8
	2.2	8.1 ± 1.0	3.7
	5	15.4 ± 0.9	2.8
	22	34.8 ± 4.5	1.6
P(DMAEMA-MAA)-AuNPs	0.5	6.1 ± 0.5	11.2
	2.2	22.6 ± 3.6	10.4
	5	69.6 ± 6.5	12.8
	22	125.6 ± 11.0	5.8
P(PEGMA-MAA)-AuNPs	0.5	1.5 ± 0.2	2.8
	2.2	3.6 ± 0.2	1.7
	5	8.8 ± 0.7	1.6
	22	29.6 ± 1.8	1.4

Figure S9. Raw SAXS data of control cells and NPs-exposed cells with corresponding error bars.

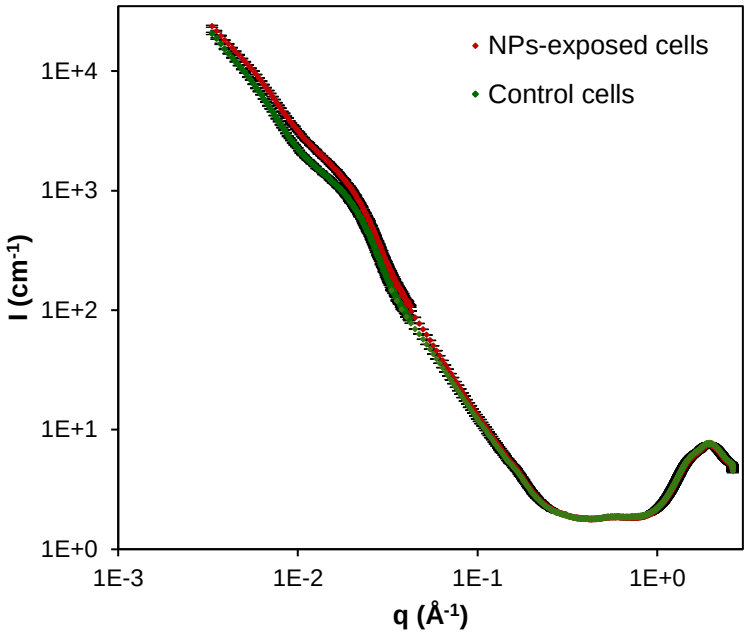

Details of invariant calculation.

After correct data treatment, we could consider the scattering signal only came from the contrast between AuNPs and the solvent, *i.e.* water. In that case, the volume fraction φ can be measured using a general property of scattering diagrams:

$$\int I(q)\, q^2\, dq = 2\pi^2\, (\Delta\rho)^2\, \varphi\, (1-\varphi)$$

where $\Delta\rho$ is the scattering length density contrast between gold and water (115 x 10^6 Å^{-2}). The term on the left-hand side is calculated from the experimental scattering diagram, and the term on the right-hand side allows to extract the volume fraction of AuNPs in the sample.

Concerning the high q domain, we extrapolated a Porod's law for NPs in incubation medium, as a decrease in q^{-4} was observed for q > 0.06 Å^{-1}. For NPs in cells, a $q^{-3.2}$ was identified, but we could not exclude that the signal did not evolve in q^{-4} at higher q. Therefore, we calculated two extreme values for this invariant, one considering an extrapolation in q^{-4} and the other considering an extrapolation in $q^{-3.2}$. In all cases, extrapolation was applied for q > 0.2 Å^{-1}.

References

1. Afssaps, *Evaluation biologique des dispositifs médicaux contenant des nanomatériaux*, 2011.
2. H. Liu, T. L. Doane, Y. Cheng, F. Lu, S. Srinivasan, J.-J. Zhu and C. Burda, *Particle & Particle Systems Characterization*, 2015, **32**, 197–204.
3. R. A. Jones, M. H. Poniris and M. R. Wilson, *Journal of Controlled Release*, 2004, **96**, 379–391.
4. S. Agarwal, Y. Zhang, S. Maji and A. Greiner, *Materials Today*, 2012, **15**, 388–393.
5. S. Hong, P. R. Leroueil, E. K. Janus, J. L. Peters, M.-M. Kober, M. T. Islam, B. G. Orr, J. R. Baker and M. M. Banaszak Holl, *Bioconjugate Chem.*, 2006, **17**, 728–734.
6. P. R. Leroueil, S. A. Berry, K. Duthie, G. Han, V. M. Rotello, D. Q. McNerny, J. R. Baker, B. G. Orr and M. M. Banaszak Holl, *Nano Lett.*, 2008, **8**, 420–424.
7. A.-K. Trützschler, T. Bus, M. Reifarth, J. C. Brendel, S. Hoeppener, A. Traeger and U. S. Schubert, *Bioconjugate Chem.*, 2018, **29**, 2181–2194.
8. A. Gallud, K. Klöditz, J. Ytterberg, N. Östberg, S. Katayama, T. Skoog, V. Gogvadze, Y.-Z. Chen, D. Xue, S. Moya, J. Ruiz, D. Astruc, R. Zubarev, J. Kere and B. Fadeel, *Scientific Reports*, 2019, **9**, 4366.
9. H. Lodish, A. Berk, S. L. Zipursky, P. Matsudaira, D. Baltimore and J. Darnell, in *Molecular Cell Biology. 4th edition*, W. H. Freeman, 2000.